Low-Sampling Frequency Two-terminal Traveling Wave-based Overhead Transmission Line Protection

F. B. Costa, J. R. Lima Júnior, M. A. Aziz Jahan, F. V. Lopes, K. M. Silva, K. M. C. Dantas

***Abstract*—Digital fault recorders (DFRs) and some conventional relays operate typically with sampling frequencies up to a few kHz. Conversely, traveling wave (TW)-based methods are usually designed to operate at sampling frequencies in the order of MHz. However, this paper demonstrates that two-terminal TW-based protection that considers the effects of the sampling frequency and TW propagation velocity uncertainties can protect transmission lines using sampling frequencies of a few kHz instead of MHz. This demonstration considers a performance validation based on challenging real-world faults recorded in transmission lines equipped with DFRs operating with a sampling frequency of 15,360 Hz. The low-sampling frequency two-terminal TW protection was implemented in hardware as a protective relay to evaluate actual data in real-time analysis, representing a significant step towards the practical application of the TW concept readily available in real protection devices with a low-sampling frequency.**

***Keywords*—Fault detection, power system protection, traveling waves.**

I. INTRODUCTION

Protection systems based on the Fourier transform, such as distance protection, differential protection, and overcurrent protection, have been traditionally used in overhead transmission lines with a sampling frequency of a few hundred Hz [1], [2]. One of the main concerns of classical protection systems is the operating time of about one cycle. However, when a fault occurs on overhead transmission lines traveling waves (TWs) propagate away toward the line terminals with a velocity close to the speed of light. Therefore, the wavefront arrival times of TWs are the first fault evidence at the line terminals and have been used to develop fast and accurate TW-based protection algorithms to overcome the limitations of traditional protection systems.

Traveling wave-based protection methods are usually divided into single- and two-terminal categories according to the number of terminals at which the fault-induced transients are analyzed [3]. Line measurements on one-terminal support methods that compare the first wavefront arrival time and those reflected from the fault point (secondary wavefront arrival time) that reach the monitored terminal [4]. However, the detection methods require more complex signal processing to detect the secondary wavefront properly and distinguish TWs reflected at the remote terminal and adjacent line terminals. Conversely, classical two-terminal TW-based protection methods are the simplest ones, because only the first wavefront arrival time at both line terminals is required [5]. However, they need communication systems and synchronization methods. The focus of this paper is on the two-terminal TW-based protection using wavefront arrival times for overhead transmission lines.

Over the last 30 years, many works have developed two-terminal TW-based protection for transmission lines [6],[7],[8]. Although the two-terminal TW-based solutions are the simplest ones, their accuracy is susceptible to uncertainties in a variety of parameters, such as the exact TW velocity estimation, whose uncertainties are mainly due to the line electrical parameters; the estimated line length; the wavefront arrival time detection, whose detection methods can provide errors due to low amplitude TWs; time synchronization through global positioning system (GPS); and fault discrimination in the presence of other high-frequency disturbances. Currently, most of these issues have been overcome. For instance, [9] presented a two-terminal-based solution without needing an external synchronization device. However, two main concerns until today in two-terminal TW-based protection methods are the requirement of sampling frequencies in the order of MHz (high-sampling frequency) and the limitation of performance validation with actual data.

The time discretization represented by the sampling frequency is one of the sources of error for TW-based methods. This issue is scarcely addressed in the literature mainly because most of the methods consider high sampling frequencies in the order of a few MHz, which minimizes the effects of time discretization. However, in 2017, [5] proposed a two-terminal TW transmission line protection considering errors associated with the sampling frequency and the TW propagation velocity estimation. This method does not need a fault location estimation and uses the speed of light in the protection algorithm to be independent of the accuracy of the TW propagation velocity estimation in overhead lines. Furthermore, [5] defined the protection zones as a consequence of the sampling process, yielding unprotected, uncertain, and protected zones. One additional contribution of [5] is the possibility of using reduced sampling frequencies when compared to MHz rates traditionally reported as an indispensable premise in literature. However, a deep proof and validation of TW-based protection with a low-sampling rate was not the focus of [5]. In addition, the main limitation of this work was that only simulation data were considered, while real-world data would be necessary for a complete evaluation and practical demonstration.

Overcoming the limitation of a TW-based method validated with only simulations is a key step toward real-life implementation. Real signals, for example, include also

Paper submitted to the International Conference on Power Systems Transients (IPST2023) in Thessaloniki, Greece, June 12-15, 2023.

high-frequency disturbances with non-stationary random waveforms that can cause malfunction of TW-based protection and fault locators applied to transmission lines [7]. For this reason, recent works have focused on validating TW-based schemes in the real-world application context. For instance, [10] assessed the performance of the methodologies proposed in [11], [12] by applying real-world fault cases. The concern with using real-world fault cases with TWs is not only restricted to academic works but also to manufacturers and developers of commercial products. For instance, [13] highlighted possibilities of protection implementations in the time domain. However, [13] only used data in a simulation environment. After that, [14] presented validation of the method with real-world faults with a high-sampling frequency.

As aforementioned, [5] demonstrated, via simulations, the possibility of using TWs to protect a transmission line by using low-sampling frequencies. [15] proposed a method for fault-induced transient detection in signals with low-sampling frequency. Therefore, by using real-world fault cases recorded at a reduced sampling frequency of 15,360 Hz instead of a few MHz, this paper demonstrates that: 1) the fault detection method proposed in [15] can accurately detect the first wavefront arrival time of TWs in a reduced sampling frequency; 2) the two-terminal TW-based protection proposed in [5] with the detection method proposed in [15] can effectively protect transmission lines by using data with a reduced sampling frequency of 15,360 Hz.

Data sampled at a high-sampling frequency will result in high protection zones by using TWs. However, as demonstrated in this paper, a reduced sampling frequency of 15,360 Hz can still result in acceptable protection zones higher than the conventional distance protection zones. Therefore, most faults can be quickly cleared using TW technology by leveraging the existing infrastructure of classic protection and monitoring systems, opening new possibilities for TW-based algorithms. For instance, digital fault recorders with a sampling frequency of 15,360 Hz (256 samples/cycle), widely used to monitor faults on transmission lines, were used to record actual data in a Brazilian power system and support this paper. The actual records include information on faults in unprotected, uncertain, and protected zones, which are critical to assess the protection method's performance under challenging situations such as close-in faults. Two TW-based relays were implemented in digital signal processors (DSPs) and connected through a communication system. The actual signals were played back to be evaluated by the TW relays in a real-time system. Implementing the TW-based protection in hardware and validation in a real-time analysis with challenging real-world fault cases with a typical sampling frequency of digital fault recorders contributes to further developing a new generation of TW-based protective relays feasible in practical terms.

II. THE TRAVELING WAVE-BASED PROTECTION

This section describes the used TW-based protection, and most equations in this section were proposed in [5].

The fault inception time t_F, unknown to the protection relays, occurs between two samplings k_F and $k_F + 1$. The sampling taken as reference k_F is the one associated with the discrete-time immediately before the fault inception time. Either the sampling before or after the fault inception time does not affect the analysis because the reference time is nullified in the classical two-terminal fault location equation. In digital sampling process at a sampling frequency f_s, the fault inception time in the continuous time t_F is converted to a discrete sampling $k_F = \lfloor t_F f_s \rfloor$, yielding:

$$k_F \leq \lfloor t_F f_s \rfloor < k_F + 1, \tag{1}$$

where $\lfloor * \rfloor$ is the largest integer value not greater than $*$ (floor function). The error ξ_{t_F} in the discrete fault inception time associated with the sampling process as follows:

$$\xi_{tF} = \lfloor t_F f_s \rfloor - k_F. \tag{2}$$

Based on (2), if $\lfloor t_F f_s \rfloor = k_F \Rightarrow \xi_{t_F} = 0$ and if $\lfloor t_F f_s \rfloor = k_F + 1 \Rightarrow \xi_{t_F} = 1$. Therefore, the error, in samples, associated with the fault inception time due to the sampling process is within the range $0 \leq \xi_{t_F} < 1$.

After the propagation time τ_{Fi}, the TWs coming from the fault point far d_{Fi} from Bus i reach the terminal i at time t_{Fi}, being partly reflected back and partly refracted beyond Bus i. The time t_{Fi} will only be detected after the TWs arrive at the bus i. Considering k_{Fi} as the first sampling after t_{Fi}, associated with the starting of the TWs at terminal i, then:

$$k_{Fi} - 1 < \lfloor t_{F_i} f_s \rfloor \leq k_{Fi}. \tag{3}$$

The error $\xi_{t_{Fi}}$ associated with the sampling of the first wavefront arrival time at the terminal i k_{Fi} is given by:

$$\xi_{Fi} = k_{F_i} - \lfloor t_{Fi} f_s \rfloor. \tag{4}$$

Considering that if $\lfloor t_{Fi} f_s \rfloor = k_{Fi} \Rightarrow \xi_{t_{Fi}} = 0$ and if $\lfloor t_{Fi} f_s \rfloor = k_{Fi} + 1 \Rightarrow \xi_{t_F i} = 1$, the error associated with the sampling process in the first wavefront arrival time at Bus i is in the range $0 \leq \xi_{t_{Fi}} < 1$.

Generalizing, for the protection device at Bus j, the error $\xi_{t_{Fj}}$ associated with the sampling process is given by:

$$\xi_{Fj} = k_{Fj} - \lfloor t_{Fj} f_s \rfloor, \tag{5}$$

where k_{Fj} is the sampling associated with the first wavefront arrival time at bus j. In the same way, the error is in the range $0 \leq \xi_{t_{Fj}} < 1$. The total error in discrete time associated with the sampling process ξ_{Fij} is given by:

$$\xi_{Fij} = \xi_{Fi} - \xi_{Fj} = k_{F_i} - k_{F_j} - \lfloor t_{Fi} f_s \rfloor + \lfloor t_{Fj} f_s \rfloor. \tag{6}$$

A. The Line Subdivision Due to the Sampling Rate

Based on the classical two-terminal fault location equation, given a transmission line with length d and the distance d_{Fi} from the fault point to the line terminal i, the difference between samples k_{Fi} e k_{Fj} can be calculated by:

$$k_{Fi} - k_{Fj} = \frac{2d_{Fi} - d}{v} f_s, \tag{7}$$

resulting in the following situations: $d_{Fi} = 0 \Rightarrow k_{Fi} - k_{Fj} = -df_s/v$, $d_{Fi} = d \Rightarrow k_{Fi} - k_{Fj} = +df_s/v$, or $d_{Fi} = d/2 \Rightarrow k_{Fi} - k_{Fj} = 0$. Therefore, internal faults are detected if

$$| k_{Fi} - k_{Fj}| < \lfloor df_s/v \rfloor \tag{8}$$

and external faults are detected if

$$\mid k_{Fi} - k_{Fj}| = \lfloor df_s/v \rfloor . \tag{9}$$

The line length is given by $d \geq v/f_s$. Thus, considering the TW propagation velocity v as a large value, low sampling frequencies can be used limited by the line length d.

For a given sampling frequency f_s, the TWs propagate a distance Δd in one sampling interval $1/f_s$ as follows

$$\Delta d = v/f_s, \tag{10}$$

where $\Delta d \leq d \Rightarrow f_s \geq v/d$. Therefore, starting from the middle of the line, each one-sample difference between both terminals detection leads to a distance $\Delta d_1 = \Delta d/2$ to each side. Therefore, from (8), internal faults can be detected if

$$-\left\lfloor \frac{d/2}{\Delta d_1} \right\rfloor < k_{Fi} - k_{Fj} < \left\lfloor \frac{d/2}{\Delta d_1} \right\rfloor, \tag{11}$$

which means that the transmission line with length d is divided in $2K$ portions of size $\Delta d_1 = \Delta d/2$ from the middle of the line, where K is defined as follows

$$K = \left\lfloor \frac{d}{\Delta d} \right\rfloor = \left\lfloor \frac{df_s}{v} \right\rfloor . \tag{12}$$

Once the line length d probably is not multiple integers of Δd, there are additional portions of Δd_2 from each line terminal defined as follows:

$$\Delta d_2 = \frac{d}{2} - \left\lfloor \frac{df_s}{v} \right\rfloor \frac{v}{2f_s}, \tag{13}$$

where $0 \leq \Delta d_2 < v/2f_s$.

B. The Protected, Uncertain, and Unprotected Zones

Based on (6) and (9), considering the error due to the sampling rate, an external fault can be identified by

$$\left|(k_{Fi} - k_{Fj}) + \xi_{t_{Fij}}\right| = \left\lfloor \frac{df_s}{v} \right\rfloor . \tag{14}$$

Hence, there is a region in the transmission line in which faults are detected as internal faults, as follows

$$D_i(t_F) < d_{Fi} < D_j(t_F), \tag{15}$$

where $D_i(t_F) = \Delta d_2 + \left|\xi_{t_{Fij}}\right| v/2$ and $D_j(t_F) = d - \Delta d_2 - \left|\xi_{t_{Fij}}\right| v/2$. Therefore, the region for internal faults changes with the error $\xi_{t_{Fij}}$, a function of the fault inception time t_F. Thus, there is an error in the fault detection associated with the sampling rate resulting in borders between internal and external faults (D_i and D_j) as a function of t_F, which are unknown distance quantities due to the unknown time t_F.

From (15), a downstream external fault is detected when

$$d_{Fi} \leq \Delta d_2 + \left|\xi_{t_{Fij}}\right| v_2 \Rightarrow d_{Fi} \leq D_i(t_f), \tag{16}$$

whereas an upstream external fault is detected when

$$d_{Fi} \geq d - \Delta d_2 - \left|\xi_{t_{Fij}}\right| v_2 \Rightarrow d_{Fi} \geq D_j(t_f). \tag{17}$$

According to (6), $\left|\xi_{t_{Fij}}\right| < 1/f_s$. Therefore, the limits of the region for internal fault detection (maximum and minimum values of D_i and D_j) are obtained with $\left|\xi_{t_{Fij}}\right| = 0$ and $\left|\xi_{t_{Fij}}\right| = 1/fs$ such as shown in Fig. 1. For instance, from

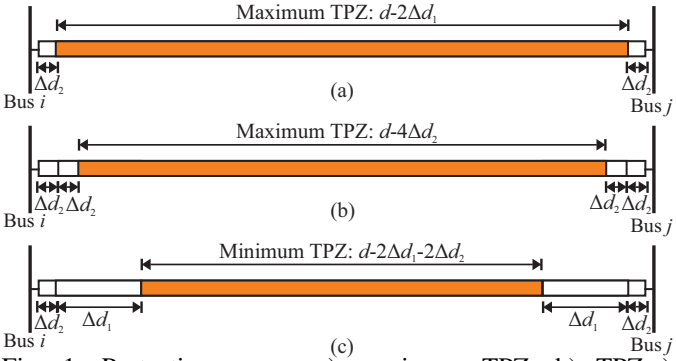

Fig. 1: Protection zones: a) maximum TPZ; b) TPZ;c) minimum TPZ.

(15), the maximum region for internal faults is obtained when $\left|\xi_{t_{Fij}}\right| = 0$ [Fig. 1(a)] as follows:

$$\Delta d_2 < d_{Fi} < d - \Delta d_2, \tag{18}$$

whereas the minimum region for internal faults is obtained when $\left|\xi_{t_{Fij}}\right| = 1/fs$ [Fig. 1(c)] as follows:

$$\Delta d_2 + \Delta d_1 < d_{Fi} < d - \Delta d_2 - \Delta d_1. \tag{19}$$

Another interesting case is when $\xi_{tF} = 0$, where $\xi_{t_{Fij}}$ defined in (6) is given by

$$\left|\xi_{t_{Fij}}\right| = \left| \frac{1}{f_s} \left\lfloor \frac{df_s}{v} \right\rfloor - \frac{d}{v} \right| = 2v\Delta d_2, \tag{20}$$

and the region for internal faults [Fig. 1(b)] is given by:

$$2\Delta d_2 < d_{Fi} < d - 2\Delta d_2. \tag{21}$$

Based on (15), faults on the zone $\Delta d_2 + \Delta d_1 < d_{Fi} < d - \Delta d_2 - \Delta d_1$ are always detected as internal faults (protected zone), whereas faults on the zones $\Delta d_2 < d_{Fi} < \Delta d_2 + \Delta d_1$ and $d - \Delta d_2 - \Delta d_1 < d_{Fi} < d$ can be detected as either internal or external faults depending on the value of t_F (uncertainty zones). In addition, faults on the zones $0 \leq d_{Fi} \leq \Delta d_2$ and $d - \Delta d_2 \leq d + Fi \leq d$ are always detected as external faults (unprotected zones). Therefore, the total protected zone ($TPZ(v)$), the uncertain zone ($UZ(v)$), and the unprotected zone ($UPZ(v)$) are defined as follows:

$$\begin{aligned} TPZ(v) &= \frac{d - 2\Delta d_1 - 2\Delta d_2}{d} 100\% \\ &= \frac{v}{f_s d} \left(\left\lfloor \frac{df_s}{v} - 1 \right\rfloor \right) 100\%, \end{aligned} \tag{22}$$

$$UZ(v) = \frac{2\Delta d_1}{d} 100\% = \frac{v}{df_s} 100\%, \tag{23}$$

$$UPZ(v) = \frac{2\Delta d_2}{d} 100\% = \left(1 - \left\lfloor \frac{df_s}{v} \right\rfloor \frac{v}{df_s} \right) 100\%, \tag{24}$$

where $f_s \geq 2v/d$ in order to present a protection zone and $f_s \geq v/d$ in order to present an uncertain zone.

According to (22)-(24), the protected, unprotected, and uncertain zones are a function of the sampling frequency and the line length. These equations are fundamental because the protection system can be designed to reach a specific

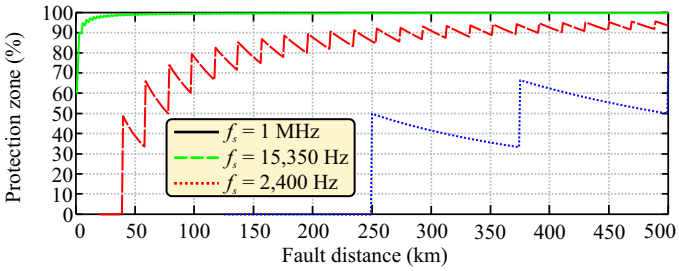

Fig. 2: Protection zones versus the line length for low- and high-sampling frequencies.

protection zone and coordinate with other protection functions. Furthermore, they enable the possibility of using a TW-based protection system with a low sampling frequency. For instance, Fig. 2 depicts the protection zone defined in (22) as a function of the line length for sampling frequencies of 2400, 15360, and 1000000 Hz (low- and high-sampling frequencies). A high-sampling frequency of 1 MHz results in outstanding protection zones higher than 98% for small and long transmission lines. Since the current technology allows practical applications of TW-based approaches at a sampling frequency of 1 MHz, this would be the best choice. Nevertheless, the definition of protection zones also allows the use of low sampling frequencies depending on the size of the line, opening new possibilities for TW-based protection, as addressed in this paper. For instance, a sampling frequency of 15,360 Hz would result in a protection zone of about 90% for lines higher than 250 km. A lower sampling frequency (e.g., 2400 Hz) could only be applied for lines with lengths higher than 250 Km, but with reduced protection zones.

III. Wavelet-based Detection Method

Two-terminal TW-based protection must detect the first wavefront arrival time. In this paper, the wavelet-based fault detection method proposed in [15] provides the first wavefront arrival time to the proposed TW-based protection method.

The first-level wavelet signals of the real-time stationary wavelet transform with border distortions are given by [15]:

$$w(l,k) = \frac{1}{\sqrt{2}} \sum_{n=0}^{L-1} h_\psi(n) \overset{\circ}{i}_\Phi(k - L + n + 1 + l), \qquad (25)$$

where $k \geqslant \Delta k - 1$ is the current index time k/f_s; $0 \leqslant l < L$ is the border index; h_ψ is the high-pass wavelet filter; L is the filter length; $\Delta k \geqslant L$ is the sliding window length; $\overset{\circ}{i}_\Phi(k+m) = i_\Phi(k - \Delta k + m)$ with $m \in \mathbb{N}^*$, which is a periodized current in Δk samples.

The wavelet coefficient energy, given by [15]:

$$\mathcal{E}(k) = \sum_{l=1}^{L-1} [w(l,k)]^2 + \sum_{n=k-\Delta k+L}^{k} [w(0,n)]^2, \qquad (26)$$

will be used for the first wavefront arrival time detection with the Daubechies wavelet filter with four coefficients by means of a hard energy increase, as addressed in Section IV.

IV. Performance Assessment with Actual Records

This paper considers challenging actual faults and hardware implementation to demonstrate that the method proposed in [5] can be used in a practical protection application in transmission lines with TW-based relays at a low-sampling frequency. The faults occurred in some transmission lines of CHESF, a Brazilian power transmission utility with over 21.000 km of AC transmission lines, at voltages of 500, 230, 138, and 69 kV and a nominal frequency of 60 Hz. The performance evaluation considered six actual faults on transmission lines with different topologies and voltage levels. Table I summarizes the transmission lines' parameters where the faults occurred.

TABLE I: Case Studies and Line Parameters

Line	kV	R^+	X_L^+	X_C^+	R^0	X_L^0	X_C^0	d
04S1	230	0.097	0.516	3.209	0.389	1.399	2.222	58.8
04F5	230	0.047	0.357	6.268	0.214	1.245	4.553	7.4
05V5	500	0.024	0.321	5.128	0.206	1.021	3.125	159.7
05L8	500	0.023	0.283	5.916	0.256	0.966	3.339	114.0
04C8	230	0.099	0.505	3.279	0.372	1.327	2.102	71.3
04L1	230	0.098	0.519	3.206	0.536	1.510	2.378	198.0

Actual DFRs with a sampling frequency of f_s=15,360 Hz recorded each fault in both line terminals following the COMTRADE standard. Therefore, twelve actual records obtained in the CHESF power system represent these six faults. The records were not synchronized. However, the line maintenance teams provided each fault with an actual fault location and cause. Therefore, the two actual records of each fault could be synchronized using linear regression. Fig. 3 shows the synchronization process used in this paper. The proposed two-terminal TW-based protection does not estimate the fault location. The actual fault location information is only used for the protection performance assessment.

The evaluation of the actual records results in identifying the discrete wavefront arrival times k_{Fi}/f_s and k_{Fj}/f_s at terminals i and j, respectively. Since the detection of TWs is beyond the scope of this paper, detecting the first wavefront arrival time in both terminals was accomplished using the wavelet transform as support to identify the instants. Based on [15], the energy of the wavelet coefficients detects fault inception time accurately.

Considering the discrete wavefront arrival times k_{Fi}/f_s and k_{Fj}/f_s obtained in the wavelet domain, actual fault location information d_{Fi} and d_{Fj} provided by the line maintenance teams, and the estimation of the line propagation velocity v based on line parameters shown in Table I, the fault inception time k_F/fs could be estimated and taken as reference for the synchronization process. The synchronization process in Fig. 3 is based on Δ_s, which is related to the difference between the fault inception times in both fault records as follows:

$$\Delta_s = \left| k_{Fi} - k_{Fj} - \left\lfloor \frac{d_{Fi} f_s}{v} \right\rfloor + \left\lfloor \frac{d_{Fj} f_s}{v} \right\rfloor \right|. \qquad (27)$$

Regarding the protection algorithm, the TW propagation velocity was considered equal to the speed of light c as proposed in [5]. Therefore, in one sampling interval $1/f_s$, TWs travel a distance of $\Delta d = 19.53$ km according to (10). From the middle of the lines, K portions of $\Delta d_1 = 9.77$ km are considered. In a more conservative way, in all cases, the minimum total protection zone was considered as calculated

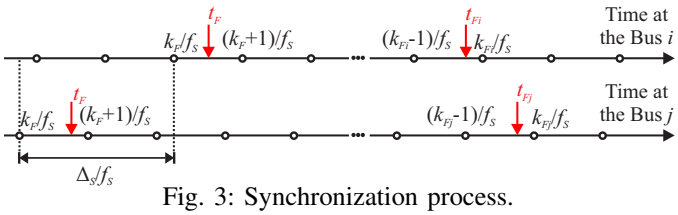

Fig. 3: Synchronization process.

in (24). Table II summarizes the theoretical protection zones, highlighting unprotected, uncertain, and protected zones of each transmission line. Among these six cases, this section will discuss the detailed results of three cases.

TABLE II: Theoretical protection zones

Line	d km	Voltage kV	UPZ km	UZ km	TPZ km	Fault km	Class
04S1	58.8	230	0.10	9.77	39.06	10.0	Internal
04F5	7.4	230	3.70	9.77	19.53	0.6	External
05V5	159.7	500	1.72	9.77	136.72	39.7	Internal
05L8	114.0	500	8.17	9.77	78.13	7.0	Internal
04C8	71.3	230	6.35	9.77	39.06	0.0	External
04L1	198.0	230	1.34	9.77	175.78	92.0	Internal

The TW-based protection proposed in [5] with the wavelet-based wavefront arrival time detection proposed in [15] were implemented in a DSP TMS320C6713 with the digital starter kit. The DSP can operate at 225 MHz and handle up to 1800 million instructions per second. Two DSPs were used in place of relays at busses i and j. The actual signals for each fault were played back to be evaluated in real-time by the DSPs at f_s=15,360 Hz. A wavelet coefficient energy required a computational burden of 10 microseconds, which is less than the sampling time of 65 microseconds. A high-speed Ethernet cable of CAT5e type with an RJ45 connector was used to establish communication between the DSPs. Then, one DSP submitted the local signals, i.e., actual signals played back to run in real-time, to the remote DSP. The delay of the communication equipment was about 3 milliseconds.

A. Case Study 1

A single line-to-ground (SLG) fault at phase C took place on line 04S1, which connects the substations FZD and CPE. A lightning discharge on the structure 10/1 located 10 km far from the substation FZD caused the fault. The traditional impedance fault locators indicated 9.59 km far from FZD substation, which is near the actual location of 10 km. Figs. 4 and 5 depict the actual currents, actual voltages, and one of the wavelet energy at the terminals FZD and CPE, respectively. These actual signals were played back in a real-time platform, and the wavelet signals were obtained in real-time analysis.

Based on the analysis in the wavelet domain, the samplings associated to the first wavefront arrival time are $k_{Fi} = 3058$ for terminal FZD and $k_{Fj} = 3055$ for the terminal CPE. The transmission line presents a single-circuit topology with a voltage 230 kV and length $d = 58.8$ km. Based on (27), the amount of samples to perform the synchronization of the records is Δ_s=1. Therefore, the sampling index associated to the first wavefront in the terminal FZD is compensated by $\Delta_s = 1$, and it is now $k_{Fi} = 3058 - 1 = 3057$.

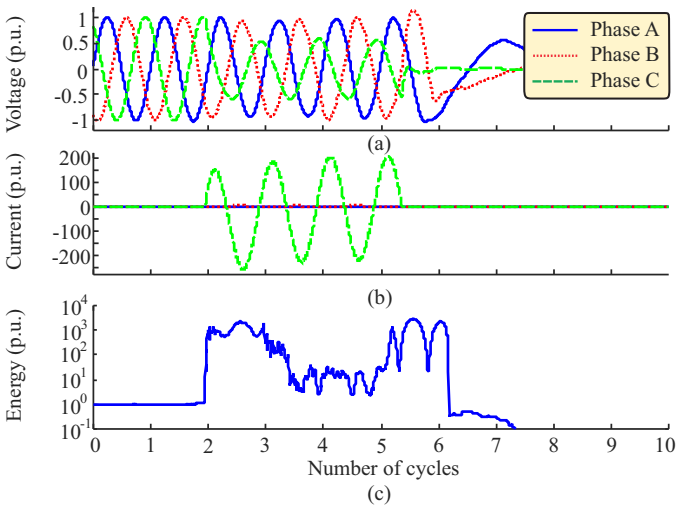

Fig. 4: Normalized actual signals, terminal FZD: a) voltages; b) currents; c) phase-A wavelet energy obtained in real-time.

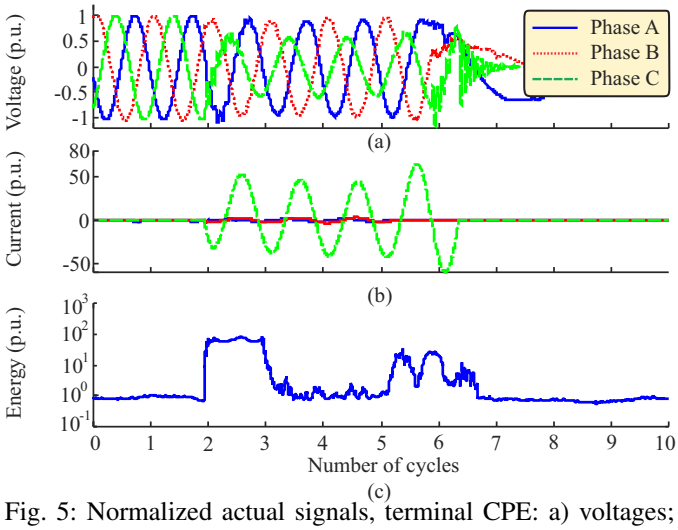

Fig. 5: Normalized actual signals, terminal CPE: a) voltages; b) currents; c) phase-A wavelet energy obtained in real-time.

Considering the effects of sampling rate, (12) yields K=3, that is, there are $3\Delta d_1$ portions from the middle of the line to each side of the line. Furthermore, $\Delta d_2 = 0.10$ km. Based on (19), faults are considered as internal ones if they are inside the protected zone, given by $9.87 < d_{Fi} < 48.93$. The unprotected zone is given by $UPZ(\%) = 0.34\%$, whereas the uncertain zone is given by $UZ(\%) = 33.23\%$ and the protected zone $TPZ(\%) = 66.43\%$.

Fig. 6 depicts the protection zones of the actual line 04S1 by considering the sampling frequency of f_s=15,360 Hz and the position of the actual fault, which was in the border of protected and uncertain zones. Therefore, in theory, it is expected to detect this fault as an internal one. The TW-based protection considers (8), which results in $2 < 3$. Therefore, since the condition in (8) has been satisfied, the protection system would detect this fault as an internal fault, and the transmission line would be protected as expected.

By using a low-sampling frequency of f_s=15,360 Hz, the TW-based protection system proposed in [5] would protect 66.43% of the line 04S1 (Fig. 6). Therefore, even using a low sampling rate if compared to the sampling rate of a few MHz

Fig. 6: Protection zones of the line 04S1 (230 kV).

used in most TW-based applications, the protection system would still protect a large region of line 04S1. The main limitation of this TW-based protection method is to detect close-in faults, which are the faults in the unprotected zone and some faults in the uncertain zone. Nevertheless, since the protection zone is well-defined, the proposed TW protection can coordinate with other protection functions to ensure the detection and clearance of close-in faults. The combination of the proposed TW-based protection with existing ones would cover the entire line and would present fast protection for faults inside the TW protection zone. Furthermore, the proposed method can also run at high sampling frequencies. For instance, if the records in Figs. 4 and 5 were recorded at 1 MHz, the protection zone of line 04S1 would be 99.5%.

The real relay with conventional protection cleared the fault after 57 and 74 ms at terminals FZD and CPE, respectively, as shown in Figs. 4 and 5. The relay operating time was about 16 ms (one cycle). By using TWs, the relay operating time in the experimental setup was less than 4 ms, considering the communication equipment and channel delays. Therefore, besides covering a great region of line 04S1, this TW-based protection function would achieve faster protection operating time than traditional phasor-based protection algorithms.

B. Case Study 2

Vegetation burning under line 05V5 induced an SLG fault in phase C far 39.7 km from substation JDM (d_{Fi}=39.7 km), close to structure 122/1, according to the line maintenance teams. The line is 159.7 km long and connects substations JDM and XGO at 500 kV. The distance protection operated correctly, opening the circuit breakers at approximately 41 ms at the JDM substation and 65 ms at the XGO substation. The fault locators at the JDM and XGO terminals indicated 30.12 km and 103.32 km, respectively. Figs. 7 and 8 depict the actual currents, actual voltages, and one of the wavelet energy at the terminals JDM and XGO, respectively. These actual signals were played back in a real-time platform, and the wavelet signals were obtained in a real-time analysis in the DSPs.

The first wavefront arrival time detected in each terminal JDM and XGO is $k_{Fi} = 2861$ and $k_{Fj} = 1394$, respectively. Based on (27), the number of samples to synchronize the records is Δ_s=1463. Thus, the sample associated with the first wavefront in the terminal JDM is compensated by $\Delta_s = 1463$ samples. Therefore, it is now $k_{Fi} = 2861 - 1463 = 1398$.

Considering the effects of the sampling frequency, (12) yields K=8, that is, there are $8\Delta d_1$ portions from the middle of the line to each side of the line. As a result, $\Delta d_2 = 1.72$ km. Based on (8), faults are considered internal ones if they are inside the protected zone, given by $11.49 < d_{Fi} < 148.21$. The unprotected zone is $UPZ(\%) = 2.15\%$, the uncertainty zone is $UZ(\%) = 12.23\%$ and the protected zone $TPZ(\%) = 85.62\%$. Fig. 9 depicts the protection zones of the actual line 05V5 by considering f_s=15,360 Hz and the position of the actual fault, within the protected zone. Therefore, it is expected the detection of this fault as an internal one.

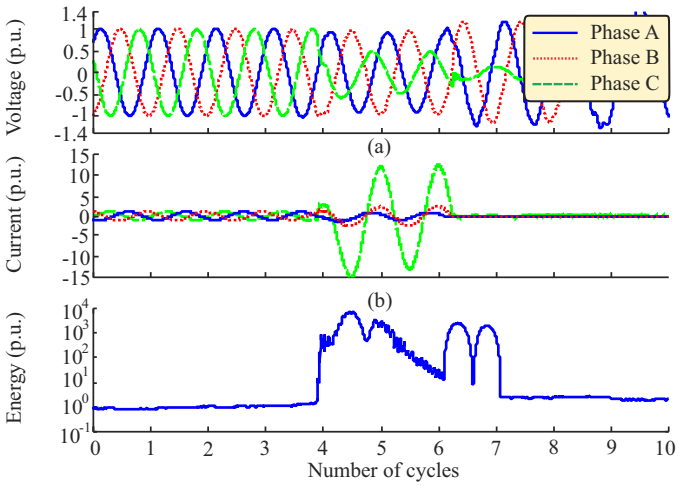

Fig. 7: Normalized actual signals, terminal JDM: a) voltages; b) currents; c) phase-A wavelet energy obtained in real-time.

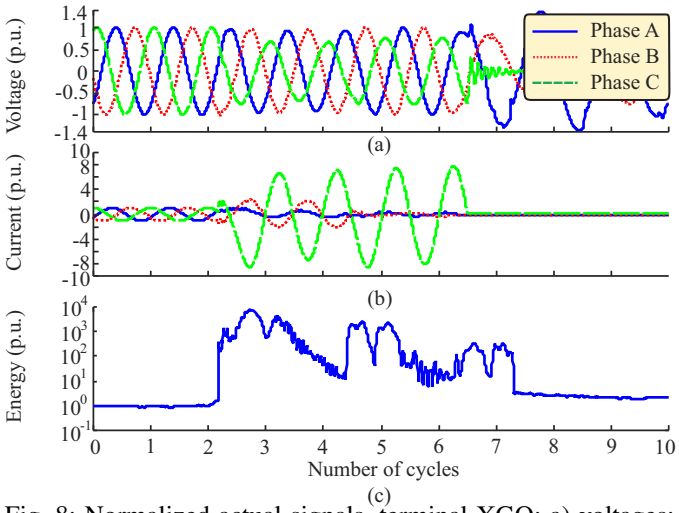

Fig. 8: Normalized actual signals, terminal XGO: a) voltages; b) currents; c) phase-A wavelet energy obtained in real time.

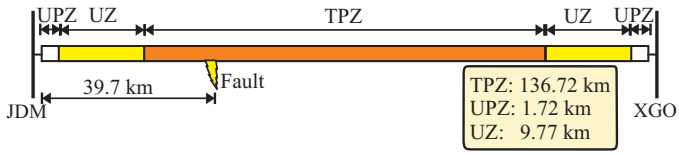

Fig. 9: Protection zones of the line 05V5 (500 kV).

The TW-based protection considers (8), which results in 4 < 8. Therefore, since the condition in (8) was satisfied, the protection system would detect this fault as an internal fault, and the transmission line would be fast-protected as expected.

The protected zone increases with the line length for a given sampling rate, indicating that this method performs better for long lines by using a low sampling frequency. For a sampling frequency of 15,360 Hz, the protected zone covered 85.62% of the line length, which is comparable to a typical setting for zone 1 distance protections. If the signals in Figs. 7 and 8 were

recorded at 1 MHz, the protection zone would be 99.75%.

Regarding the relay operating time, the real relay with conventional protection cleared the fault after 40 and 72 ms at terminals JDM and XGO, respectively, with a relay operating time of about 16 ms (one cycle). By using TWs, the relay operating time in the experimental setup was less than 4 ms.

C. Case Study 3

An explosion of the lightning arrester at the substation RCD caused an SLG fault in phase C of transmission line 04C8. The lightning arrester position is after the current transformer, therefore inside the transmission line. This paper considers the fault location at d_{Fi}=0, i.e., at the beginning of the line. Therefore, it is a close-in fault placed inside the unprotected zone. The phasor-based fault locator on the RCD terminal indicated a fault distance of 130 m, therefore with acceptable precision. The transmission line 04C8 has a length of d=71.3 km and connects the substations RCD and GNN. Figs. 10 and 11 depict the actual currents, actual voltages, and one of the wavelet energy at the terminals RCD and GNN, respectively. These actual signals were played back in a real-time platform, and the wavelet signals were obtained in real-time analysis.

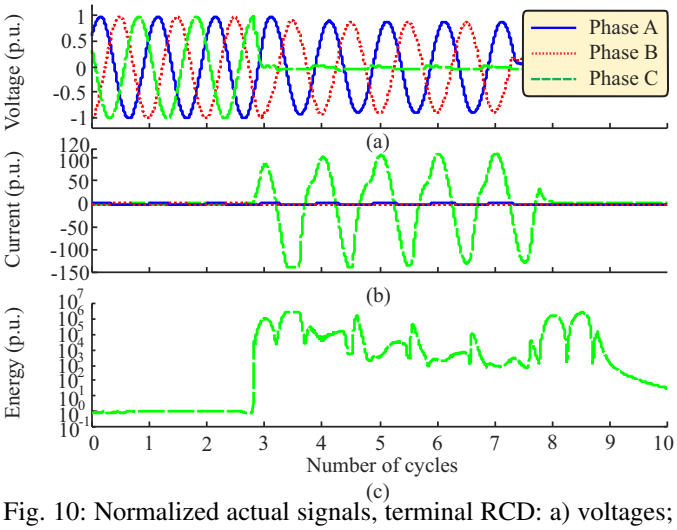

Fig. 10: Normalized actual signals, terminal RCD: a) voltages; b) currents; c) phase-C wavelet energy obtained in real time.

The first wavefront detected in each terminal is k_{Fi}=3026 for terminal RCD and k_{Fj}=3022 for terminal GNN. Therefore, according to (27), the synchronization process considers Δ_s=0. Thus, there is no need to compensate for synchronization in these records.

Considering the effects of the sampling process, (12) yields K=3, that is, there are $3\Delta d_1$ portions from the middle of the line to each side of the line. So, $\Delta d_2 = 6.35$ km. Based on (8), faults are considered internal ones if they are within the protected zone, given by $16.12 < d_{Fi} < 55.18$. The unprotected zone is $UPZ(\%) = 17.8\%$, the uncertain zone is $UZ(\%) = 27,4\%$ and the protected zone $TPZ(\%) = 54.8\%$. Fig. 12 depicts the protected, uncertain, and unprotected zones of the actual line 05V5 by considering the sampling frequency f_s=15,360 Hz and the position of the actual fault, which was within the unprotected zone. Therefore, it is expected the detection of this fault as an external one.

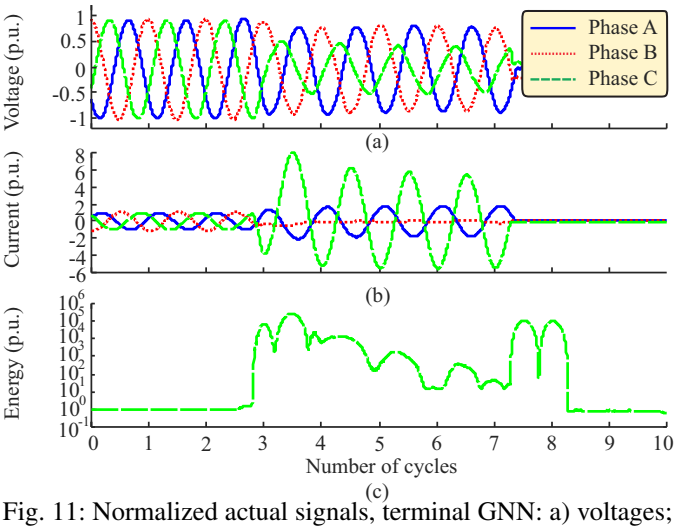

Fig. 11: Normalized actual signals, terminal GNN: a) voltages; b) currents; c) phase-C wavelet energy obtained in real time.

Fig. 12: Protection zones of the line 04C8 (230 kV).

The TW-based protection considers (8), which results in 4 < 3. Therefore, (8) was not satisfied, and the fault was considered an external one, as expected. If the records shown in Figs. 10 and 11 were recorded at 1 MHz, the protection zone of line 04C8 would be 99.30%. In this case, the fault would be detected as external, even using a high sampling rate.

As pointed out before, close-in faults or faults located in the uncertainty region are considered as external ones in this protection function because it is not possible to distinguish correctly between internal and external faults due to the sampling process effect. For close-in faults, as discussed, it is necessary to adopt the usual protections associated with the TW-based ones to protect the entire transmission line.

Regarding the relay operating time, the real relay with conventional protection cleared the fault after 83 and 76 ms at terminals RCD and GNN, respectively, with a relay operating time of about 16 ms (one cycle). By using TWs, the relay operating time in the experimental setup was less than 4 ms.

V. Qualitative Comparison Against Existing Superimposed Quantity-Based Protections

Over the past years, several high-speed protection elements have been proposed, among which those based on superimposed components stand out [4], [13], [14]. Superimposed signals have a wide spectrum, such that low and high-frequency bands have been used to implement a number of protections, such as, for example, directional and differential elements. Directional elements based on the spectrum inferior part are often called TD32, whereas those based on the spectrum superior band analyzing TWs are frequently called TW32. In turn, differential elements based on TWs are often called TW87.

To provide a qualitative comparison between the above-mentioned functions and the proposed algorithm,

few features of each approach are highlighted. The TD32 function requires sampling rates in the order of a few tens of kilohertz, being capable of distinguishing forward from reverse faults in a few milliseconds. Conversely, TW32 is based on the analysis of the first incident TWs that reach the monitored buses, such that it distinguishes forward from reverse faults in a few microseconds. The TW87 is also very fast, but it requires the detection of exit TWs [13], [14], so that there is an intrinsic delay in the order of the line travel time for close-in and far-end faults. All these functions need communication channels to implement unit protection schemes. Moreover, TD32 and TW32 need to monitor both voltage and current signals. However, since TD32 and TW32 analyze only relative polarities, time synchronization is not an issue. In turn, time alignment is mandatory for the TW87.

The proposed solution depends on communication channels and time synchronization. However, it analyzes only the first transients at both line ends, and monitoring voltage signals is not required since it can properly work with only currents. Thus, it is an alternative for cases in which voltage measurements are not available, either due to problems in potential transformers (PTs) or unavailability of PT secondary windings. In addition, it is based on a widespread two-terminal TW-based line monitoring technology, which facilitates its application in existing power systems.

VI. CONCLUSION

This paper demonstrates through challenging actual faults and hardware implementation that a two-terminal traveling wave-based protective device can properly operate at a sampling frequency of 15,360 Hz instead of a few MHz. The performance evaluation of this protection function with challenging real-world data played back in a real-time platform demonstrated the effectiveness of this traveling wave-based protection method and its feasibility in real applications.

The evaluated two-terminal traveling wave-based protective device considers the effects of the sampling process and traveling wave propagating velocity uncertainties. As a consequence, protected, unprotected, and uncertain zones could be defined in theory. The actual records with faults used in this paper contained situations where faults occurred in these three zones. Therefore this paper validated the theory with realistic data streams providing a key contribution in demonstrating that two terminal traveling wave-based protection can adequately protect overhead transmission lines in practical applications by using a sampling frequency of 15,360 Hz, especially in long lines.

The advantage of traveling wave-based protection with low-sampling frequencies to protect overhead transmission lines is that it will require an infrastructure similar to that used by most traditional protections. Furthermore, after identifying the errors associated with the traveling wave velocity estimation and the effects of the sampling frequency in overhead transmission lines, the analysis performed in this paper showed that the adoption of the speed of light as propagation speed is acceptable, making the method independent from line parameters.

The main disadvantage of two-terminal traveling wave-based methods using the first wavefront arrival times is the detection of close-in faults. However, by including the effects of the sampling process of digital signals, the proposed method identified unprotected zones, which are ranges where close-in faults are not detected. Identifying the unprotected zones may enable the coordination of this protection with existing ones to detect close-in faults.

As a further development, the proposed traveling wave-based method will consider the protection of transmission lines with the integration of inverter-based resources, such as wind energy conversion systems. Furthermore, a comprehensive comparison with the existing TD32, TW32, and TW87 is also proposed as further work for identifying advantages, disadvantages, and coordination among them.

REFERENCES

[1] C. Venkatesh and K. S. Swarup, "Investigating performance of numerical distance relay with higher sampling rate," in *2012 North American Power Symposium (NAPS)*, 2012, pp. 1–6.

[2] E. Schweitzer and D. Hou, "Filtering for protective relays," in *IEEE WESCANEX 93 Communications, Computers and Power in the Modern Environment - Conference Proceedings*, 1993, pp. 15–23.

[3] P. F. Gale, P. A. Crossley, X. Bingyin, G. Yaozhong, B. J. Cory, and J. R. G. BArker, "Fault location based on travelling waves," *Fifth International Conference on Developments in Power System Protection*, vol. 15, 1993.

[4] R. L. d. S. França, F. C. d. S. Júnior, T. R. Honorato, J. P. G. Ribeiro, F. B. Costa, F. V. Lopes, and K. Strunz, "Traveling wave-based transmission line earth fault distance protection," *IEEE Transactions on Power Delivery*, vol. 36, no. 2, pp. 544–553, 2021.

[5] F. B. Costa, A. Monti, F. V. Lopes, K. M. Silva, P. Jamborsalamati, and A. Sadu, "Two-terminal traveling-wave-based transmission-line protection," *IEEE Trans. Power Del*, vol. 32, no. 3, p. 1382–1393, 2017.

[6] O. Naidu, , and A. K. Pradhan, "A traveling wave based fault location method using unsynchronized current measurements," *IEEE Trans. Power Del*, vol. 34, no. 25, pp. 505–513, 2019.

[7] M. Parsi and P. Crossley, "Optimised time for travelling wave fault locators in the presence of different disturbances based on real-world fault data," *IEEE Open Access Journal of Power and Energy*, vol. 8, pp. 138–146, 2021.

[8] M. Gilany, D. khalil Ibrahim, and E. S. T. Eldin, "Traveling-wave-based fault-location scheme for multiend-aged underground cable system," *IEEE Trans. Power Del*, vol. 22, no. 1, pp. 82–88, 2007.

[9] F. V. Lopes, D. Fernandes, and W. L. A. Neves, "A traveling-wave detection method based on park's transformation for fault locators," *IEEE Trans. on Power Delivery*, vol. 28, no. 3, pp. 1626–1634, 2013.

[10] F. V. Lopes, P. Lima, J. P. G. Ribeiro, T. R. Honorato, K. M. Silva, E. J. S. Leite, W. L. A. Neves, and G. Rocha, "Practical methodology for two-terminal traveling wave-based fault location eliminating the need for line parameters and time synchronization," *IEEE Trans. Power Del*, vol. 34, no. 6, pp. 2123–2134, 2019.

[11] F. V. Lopes, "Settings-free traveling wave based earth fault location using unsynchronized two-terminal data," *IEEE Power Energy Society General Meeting (PESGM)*, pp. 1–1, 2018.

[12] F. V. Lopes, K. M. Dantas, K. M. Silva, and F. B. Costa, "Accurate two-terminal transmission line fault location using traveling waves," *IEEE Trans. Power Del*, vol. 33, no. 2, pp. 873–880, 2018.

[13] I. Edmund O. Schweitzer, B. Kasztenny, A. Guzmán, V. Skendzic, and M. V. Mynam, "Speed of line protection – can we break free of phasor limitations?" *2015 68th Annual Conference for Protective Relay Engineers*, pp. 448–461, 2015.

[14] I. Edmund O. Schweitzer, B. Kasztenny, and M. V. Mynam, "Performance of time-domain line protection elements on real-world faults," *2016 69th Annual Conference for Protective Relay Engineers (CPRE)*, pp. 1–17, 2016.

[15] F. B. Costa, "Fault-induced transient detection based on real-time analysis of the wavelet coefficient energy," *IEEE Transactions on Power Delivery*, vol. 29, no. 1, pp. 140–153, 2014.